Wire-EDM geometrical simulation based on superposition of single craters

Author(s):
Borges, Paulo; Hensen, Micha; Marra, Lucas; Kuffa, Michal; Wegener, Konrad

Publication date:
2023

Permanent link:
https://doi.org/10.3929/ethz-b-000642003

Originally published in:
Procedia CIRP 117, https://doi.org/10.1016/j.procir.2023.03.042

Available online at www.sciencedirect.com

ScienceDirect

Procedia CIRP 117 (2023) 243–248

www.elsevier.com/locate/procedia

19th CIRP Conference on Modeling of Machining Operations

Wire-EDM geometrical simulation based on superposition of single craters

Paulo Borges*[a], Micha Hensen[a], Lucas Marra[a], Michal Kuffa[a], Konrad Wegener[a]

[a]*Institute of Machine Tools and Manufacturing, ETH Zentrum LEE Leonhardstrasse 21, 8092 Zürich, Switzerland*

* Corresponding author. Tel.: +41 44 633 08 19. E-mail address: borges@iwf.mavt.ethz.ch

Abstract

Setting EDM technology parameters is a time consuming and expensive process. The development of a process model facilitates the understanding of the input parameters on the process results, which can speed up the selection of the optimal technology for a cut. This work aims to model the wire-EDM machining process with a three-dimensional geometrical voxel model through the sequential placement of single craters. To model workpiece sizes closer to reality, 2.25 10^9 voxel elements are used to construct the virtual workpiece. The simulation showed that under the same pulse energy conditions, main cut simulations have a smaller average roughness compared to trim cuts, a claim that is supported by experiments presented in this work. This disparity is related to the direction of the craters imposed by the geometrical conditions, i.e. the position of the wire relative to the workpiece. Furthermore, the simulation showed proportional roughness values compared to the experimental ones, though always underestimating the roughness value. This difference emerges because the model, as it does not incorporate the build up around the craters that might appear on the surface.

Keywords: Electrical Discharge Machining (EDM); Geometrical Simulation; Voxel Simulation

1. Introduction

Wire Electrical Discharge Machining (Wire-EDM) is a non conventional manufacturing process that cuts electrically conductive material independent of its hardness. The material is removed without physical contact, instead the process is based on a series of electrical discharges between the wire and the workpiece. A voltage is applied between them, if the electric field is strong enough, the dielectric will break down and a discharge will take place. Each discharge leaves a small crater on both the tool and the workpiece. At the end, the new formed surface is composed by the superposition of successive craters, formed from electrical discharges between the two electrodes. These discharges occur at a high frequency.

While a lot of work has been done to improve the understanding of the EDM process in several areas comprehensive modeling efforts are fewer in comparison. Okada *et al.* [1] have studied spark distribution and wire vibration in wire-EDM with the help of high-speed cameras by varying the servo voltage, pulse interval time and wire running speed. Macedo *et al.* [2] investigated the electrical breakdown mechanism and identified the elements that compose the plasma by emission spectroscopy, they have also analyzed the crater formation and material removal rate under vacuum breakdown in small gaps. Liu and Guo [3] presented a numerical approach to analyze the formation of white layer (WL) and heat affected zone (HAZ). They have also reported that depending on the temperature reached, the part of the molten material will re-solidify on the surface and might form a porous white layer. Peterson *et al.* [4] tried to optimize the discharge energy for cemented carbides such that the surface integrity is not deteriorated.

Izquierdo *et al.* [6] developed a numerical finite difference model of the EDM process incorporating the effect of multiple discharges. They have also estimated plasma diameter, energy transferred, and material removal efficiency through inverse identification. Feng *et al.* [7] characterized three-dimensional features of craters, such as build up rim around the crater and the asymmetrical bowl-shape. They achieved this by modifying some spherical equations with sinusoidal, exponential and constant parameters. Turning them into non-uniform equations. Their models represented major features of single craters and crater clusters in micro-EDM.

Maradia [5] raises some reasons for the difficulty to model the whole process: the phenomena inside the plasma are not

10.1016/j.procir.2023.03.042

well understood, the stochastic nature of the process, and the small length and time scale of the process.

While several studies have focused on exploring the single crater phenomenon, a basic element for the process, little attention has been given to the geometrical consequences of the crater superposition. Since the Wire-EDM process is a sequential process this is a relevant aspect. The position of the next spark depends on the previous spark, because it has modified the workpiece geometry.

Hinduja and Kunieda [8] have presented a generalized flowchart for the whole EDM process, which is composed of 7 sections: discharge location; simulation of EDM arc plasma; temperature distribution; simulation of material removal due to single discharge; simulation of the flow field in the gap: bubbles, debris, dielectric liquid and forces acting on electrodes; simulation of the geometry; and the machine control.

Geometrical simulation

To further explore the iterative aspect of the process, because each crater modifies the surface. A model version for a wire-EDM simulation with 3 sections can be drafted. The model starts by determining a starting position for the wire and its path; if the wire has not reached the simulation end point, the position of the next crater is found, a crater is drawn from a database; if the distance of the found position is smaller than a given gap distance, the crater is placed on the workpiece, else the wire moves on the path. The scheme of this geometrical model can be seen in figure 1:

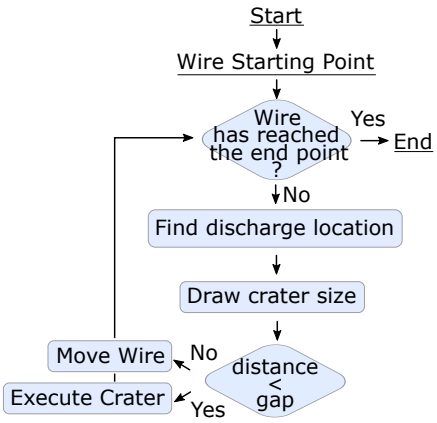

Fig. 1. Wire-EDM simulation flowchart

Discharge Location

Any simulation of the EDM process has to define a discharge location. It has been shown that the discharge location is not a deterministic process, but rather a stochastic phenomenon. In other words, the discharge will not always take place at the narrowest point between the two electrodes. Kunieda and Nakashima [9] have performed experiments to determine the factors that affect the discharge location. They noted that without sufficient time for deionization between sparks the consecutive pulse is strongly affect by the previous discharge. To avoid unstable cutting behavior a waiting period of at least $6\mu s$ is necessary. They have also pointed out that the debris generated around the first spark do not affect the position of the follow up discharge once few discharges are placed, but as soon as a longer series of discharges take place, the debris concentration gains relevance.

Schumacher [10] has raised the topic about the constitution of the dielectric in between the electrodes. The gap between the die sinking electrodes is clearly not filled with just dielectric liquid, but rather with bubbles and debris particles from the previous discharges. Thus brings other levels of complexity and make the determination of the spark position even more difficult.

Morimoto *et al.* [11] has attempted to advance in this field by developing a simulation method, in which the discharge location is determined through probability curves. It is assumed by them that the discharge delay time follows an exponential distribution. After establishing the model for the ignition delay time distributions, a value is drawn for all the regions a spark could take place, and the location of the discharge is given by the shortest discharge delay time. Such an approach is also convenient for the tool feed, as the movement of the tool electrode is commonly based on the ignition delay time.

Simulation of removal due to single discharge

Since the crater formation is mainly a thermal process, it is natural to use a thermal analysis to study the development of a single craters. A deeper understanding of the arc plasma is fundamental for such analysis as the definition of the boundary conditions are crucial. It is necessary to define the temperature distribution inside the plasma, the size of the heat source, the external pressure, fluid flow, etc. Besides all that, the mass, energy, and momentum equations need to be solved with moving boundaries.

Additionally, the process is geometric dependent. The electrodes' topography also influences the location and evolution of the discharge. Such a problem requires an iteratively approach to be solved. Making an accurate simulation of the removal due to a single discharge considerably difficult.

Nevertheless, several simulations of material removal and crater formation can be found in the literature. Shao and Rajurkar [12], for example, use an electro-thermal model to simulate the formation of a single crater. They have assumed a gaussian distributed heat flux, temperature dependent thermal properties for the materials and an expanding plasma radius. Those boundary conditions are usually found in thermal simulations but are not available and have to be most of the times assumed. Their crater dimensions are determined by the isothermal line which corresponds to the melting temperature. But this line does not correspond to the observed craters. In order to have a more realistic result, a molten material removal efficiency correction is added.

Yang et. al [13] have taken another approach, they have simulated the formation of single craters in micro-EDM in three dimensions using molecular dynamics. This is a feasible approach for the micro-EDM range, crater diameters in the range of 100 Å and discharge durations in the tenths of picoseconds. In their simulation, the material removal mechanism is due mainly to metal vaporization and explosion of superheated

metal. Their simulation has indicated a metal removal efficiency between 0.02 and 0.05, which leaves most of the melt pool for resolidification.

A shortfall of most models is that they end up creating symmetrical and circular craters. Borges *et al.* [14] have reported non circular single craters when studying the effects of wire diameter and the spark energy on the craters' dimensions. They have observed that after a given energy value, the shape of the crater ceases to be stochastic and becomes systematically elongated. This effect has shown to be more pronounced with the further increase of the pulse energy and decrease of the wire diameter. Such phenomenon is intrinsically connected with the the gap between the two electrodes.

Machine Control

Over the last years, many different control strategies have been proposed to improve the feed rate control of WEDM machines, which is customarily based on the ignition delay time. The different complex phenomena that occur during the erosion process and its stochastic nature make the process difficult to model mathematically. Therefore, during the last two decades there has been a trend of attempting adaptative fuzzy control strategies. For example, Hoseinnezhad *et. al* [15] presented a method to control the gap distance using a type-2 fuzzy logic inference system, with claimed robustness to variations in machining conditions and enhanced accuracy in a simulation. Almeida *et al.* in [16] wrote a detailed overview of the historical development of control strategies of the servo control for WEDM machines, emphasizing heuristic fuzzy control algorithms [17, 18, 19], or simple support vector machines [20].

2. Geometrical model

The presented simulation aims to explore the geometrical consequences of placing the craters. Since the process depends on the geometry, which changes with each discharge. Such aspect can only be explored by a simulation.

2.1. Voxel Model

In this simulation, the workpiece is modeled with voxels (volumetric pixels). The workpiece is a block (12.5*mm* x 0.3*mm* x 0.3*mm*) modeled with voxels (0.5μm x 0.5μm x 2μm) figure 2 shows the workpiece schematically. The workpiece is represented by 2.25 10^9 voxel elements. The choice for the length in the x and y directions, 0.3*mm*, is related to the wire diameter used, 0.2*mm*. The length in the z-direction is related to the minimum amount necessary to extract the average roughness. For the average roughness, between 2 μm and 10 μm, an evaluation length of 12.5*mm* is recommended by the EN ISO 4288 norm.

2.2. Single Craters

To draw a crater size for the simulation, an experimental database was created. Several single craters were produced, and had their geometry extracted similarly to how it is described in [14].

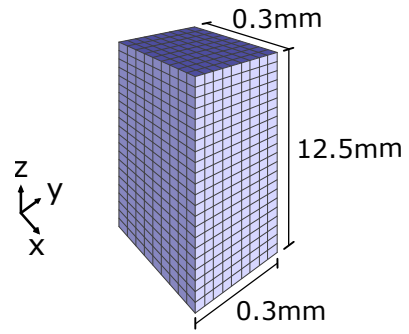

Fig. 2. Illustration of the workpiece built with voxels

To compose the database, the experiments were performed on steel 1.2379, its chemical composition is found in the following table 1. To produce the single craters, the surface of the material is machined with the wire-EDM machine itself until a smooth surface is reached (R_a = 0.3μm). Afterwards, the wire is made to pass in front of this surface with an increased gap, which restricts the number of sparks and culminate in the production of single craters.

Table 1. Steel 1.2379 chemical composition

C	Si	Mn	Cr	Mo	V
1.55%	0.30%	0.30%	11.30%	0.75%	0.75%

With the aid of an optical microscope, the topography of the craters is mapped, its dimensions are captured by fitting an ellipsoidal equation on the craters. The choice for an ellipsoidal equation allows for capturing some of the existing crater asymmetry. Figure 3 shows a image of the single craters produced.

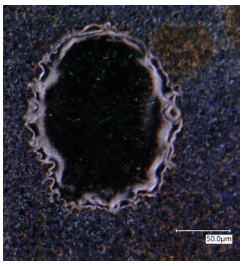

Fig. 3. Image of a single crater that composes the database

This whole procedure is done for 4 different pulse energy levels. The energy levels used for mapping the craters and the number of observations that compose the database is found in table 2.

Table 2. Pulse energies used and number of single craters observed

Pulse energies	Number of observations
5.6 *mJ*	72
15.0 *mJ*	77
17.5 *mJ*	73
19.0 *mJ*	81

To perform the erosion during the simulation, it is just necessary to randomly select a crater geometry from the database and place it on the workpiece.

It is worth mentioning that the crater model is not capable of reproducing the rim build up. The model incorporates only the material removed.

2.3. Discharge location and machine control

The discharge location is determined by the closest point between the workpiece and the wire. Such a simple rule does not encompass the complexity of the process, but is still sensitive to the surface modifications that alter the process itself.

If the distance of the closest point is smaller than a given gap value, which is set to be $20\mu m$, the point becomes the center of the ellipsoid, which was randomly selected from the database, and all the voxels inside of it are set to contain no material.

If the closest point lies outside of this gap region, i.e. the distance is bigger than the given gap value, no valid position is found and the wire should move along its path until the end of the simulation.

2.4. Wire path

Another information necessary for the simulation is the wire path. Two different wire paths were programmed: a main cut and a trim cut. The whole set up is illustrated in figure 4. To simulate the main cut, the center of the wire is positioned in the middle of the workpiece ($0.150mm$; $-0.300mm$), and made to cross the workpiece in the y-direction. Likewise for the trim cut, the center of the wire is placed at ($0.375mm$; $-0.300mm$) and made to cross the workpiece in the y-direction. For the trim cut, there is an overlap of just $0.025mm$ between the edge of the wire and the workpiece. Since the wire is represented by a cylinder of $0.20mm$ diameter.

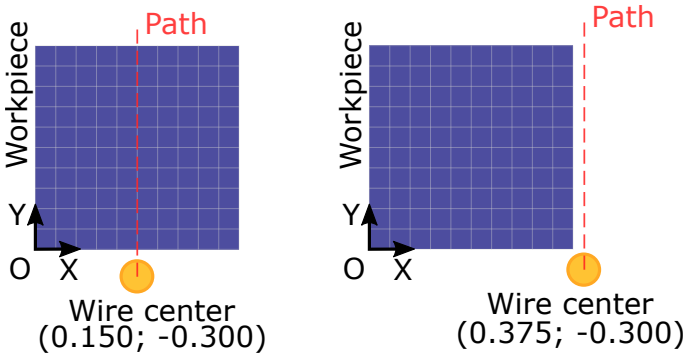

Fig. 4. On the left: Illustration of the wire path for the main cut simulation; On the right: Illustration of the wire path for the trim cut simulation

2.5. Results and discussion

At the end of the simulation, an eroded surface is left. Figure 5 shows details of the eroded surface after the simulation.

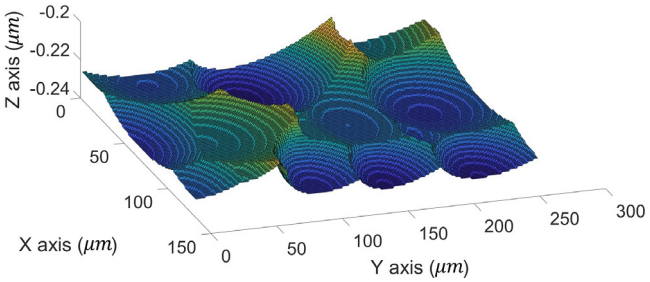

Fig. 5. Detail of a simulated eroded surface

A surface profile at the middle of the cut is extracted for roughness analysis for both main and trim cut cases. The following figure 6 shows the obtained roughness values for each pulse energy used in the simulation.

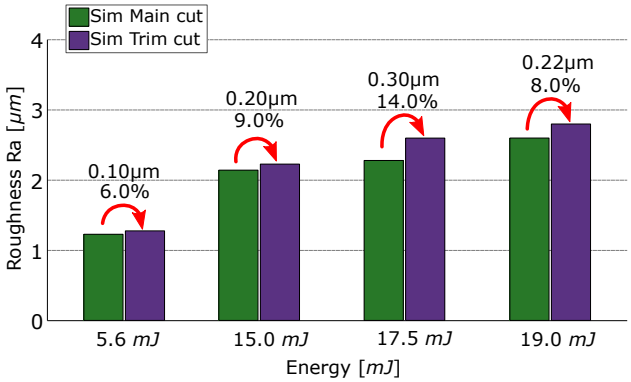

Fig. 6. Comparison of the average roughness values through the 4 different energy levels for the main cut and trim cut conditions.

Firstly, the roughness of the trim cuts have shown to be systematically higher. Analyzing the simulation, it becomes clear that this pattern is linked to the position in which the craters were placed. During the main cut, craters are placed in several directions almost all around the wire. There are frontal craters, aligned to the direction of the cut, which contribute more to the erosion of the workpiece; and there are lateral craters, perpendicular to the direction of cut, which contribute more to the final shape of the freshly eroded surface. Therefore, under main cut conditions, the eroded surface has contributions from craters positioned on a wide range of angles on the wire. Figure 7 shows one instant of the simulation of a main cut geometry with illustrations of frontal and lateral sparks.

Secondly, with an increase of the energy, there is an increase in the average roughness value, except for the $19.0mJ$ simulation. Even though the energy of the pulses are bigger, the difference between main cut and trim cut is smaller.

This may very well arise from the randomness of the process, since the craters are randomly picked from the database, or due to differences in the craters' shape in the database.

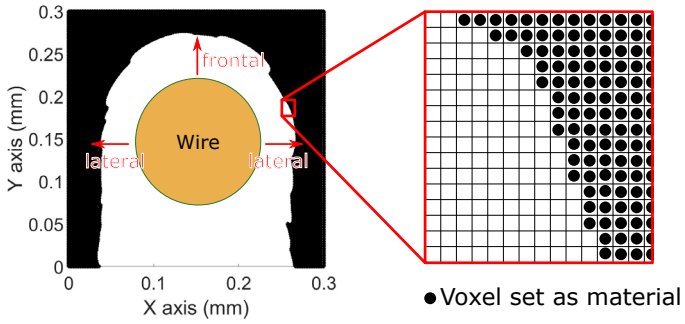

Fig. 7. On the left: a cross section of the simulation under main cut condition with indications of frontal and lateral sparks. On the right: Details for the voxels in the model

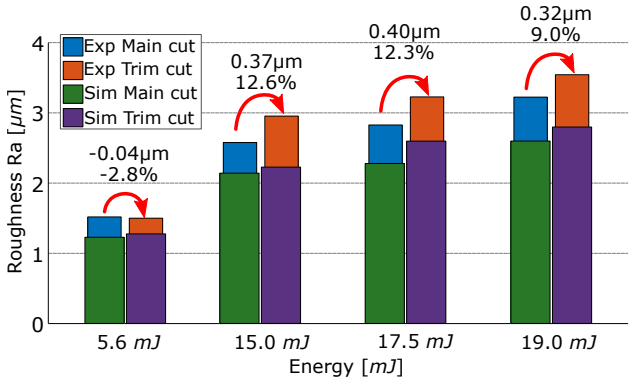

Fig. 9. Comparison between experimental and simulated roughness (Ra)

2.6. Validation

For the validation, experiments under the same geometrical conditions were performed on 1.2379 steel, same material used to map the crater sizes, and at the 4 given energy levels. Figure 8 shows the pieces after the experiments with the main cut and trim cut sections indicated.

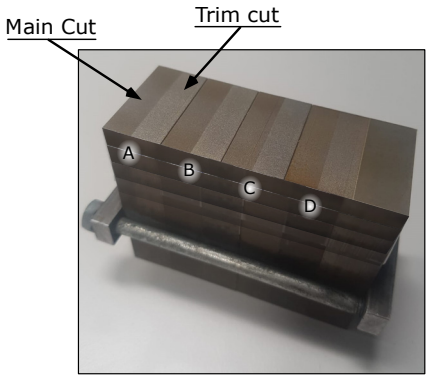

Fig. 8. Validation piece. A section corresponds to 5.6mJ energy pulse; B section corresponds to 15.0mJ energy pulse; C section corresponds to 17.5mJ energy pulse; D section corresponds to 19.0mJ energy pulse

The roughness was extracted from the segments with the help of a profilometer, Form Talysurf. Figure 9 shows the comparison between the experimental and simulated roughness values and the difference between main cut and trim cut conditions for the experiments.

It can be noted that the experimental values follow a similar trend as the simulation. The main cut exhibits a smaller average roughness value when compared to the trim cuts. The only exception happens at 5.6mJ energy, in which the trim cut had an average roughness 0.04μm smaller than the one from the main cut. Such a small value could arise from the randomness of the process and does not repel the main tendency.

The Abbott-Firestone curve, which describes the surface texture, is the cumulative density function of the surface profile.

The figure 10 shows the Abbott-Firestone curves for energy 15.0mJ under main cut conditions.

While figure 11 show the Abbott-Firestone curves for the same energy 15.0mJ under trim cut conditions.

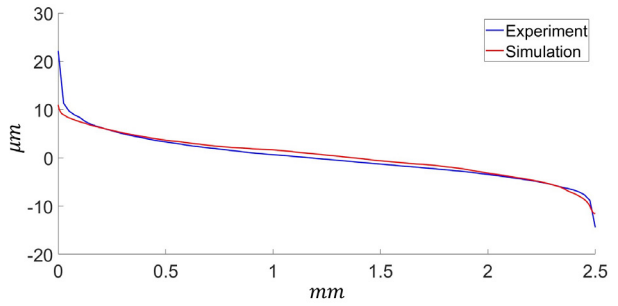

Fig. 10. Abbott-Firestone curve for the simulation and experimental results under main cut conditions for 15.0mJ of pulse energy

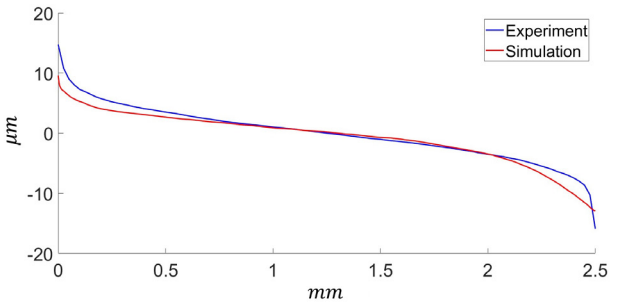

Fig. 11. Abbott-Firestone curve for the simulation and experimental results under trim cut conditions for 15.0mJ of pulse energy

While the simulation seems to adequately model the middle of the curves, a small mismatch is observed at the edges of the curve, particularly under the trim cut conditions. It implies that the model has difficulties reproducing the peaks and valleys of the surface.

This mismatch of the peaks is related to the lack of a rim build up during the simulation, since the crater's model is not capable of capturing this aspect. While the mismatch of the valley could be related to pores on the surface, which is another surface characteristic that the simulation does not encompasses. Those two points help to explain why the simulation captures the difference between main and trim cut conditions while invariably underestimating the roughness values.

3. Conclusions

Often the EDM models in the literature ignore geometrical consequences that arise from the surface modification done by previous sparks. The geometrical simulation presented in this study aims to explore this iterative aspect of the process.

The simulation, with the corroboration of experiments, has shown that the average roughness under trim cut conditions is systematically larger compared to the one under main cut conditions. This disparity exists because the surface generated under trim cut conditions has a geometrical restriction related to the direction of the craters, i.e. more lateral craters end up composing the eroded surface. While under main cut conditions, the range of crater direction in more diverse.

Additionally, a comparison between the Abbott-Firestone curves from simulation and experiments has shown a good agreement, except at the edges of the curves. It means that the simulation fails to reproduce the peaks and valleys of the real surface. This is intrinsically connected with the lack of a build up in the crater model and possible pores that appear on the surface. It explains the consistent underestimation of the roughness values.

References

[1] A. Okada, Y. Uno, M. Nakazawa, T. Yamauchi, Evaluations of spark distribution and wire vibration in wire EDM by high-speed observation, CIRP Annals, Volume 59, Issue 1, Pages 231-234, 2010.

[2] F.T.B. Macedo, M. Wiessner, C. Hollenstein, F. Kuster, K. Wegener, Dependence of Crater Formation in Dry EDM on Electrical Breakdown Mechanism, Procedia CIRP, Volume 42, Pages 161-166, 2016.

[3] J.F. Liu, Y.B. Guo, Modeling of White Layer Formation in Electric Discharge Machining (EDM) by Incorporating Massive Random Discharge Characteristics, Procedia CIRP, Volume 42, 2016, Pages 697-702.

[4] T. Petersen, U. Küpper, A. Klink, T. Herrig, T. Bergs, Discharge energy based optimisation of sinking EDM of cemented carbides, Procedia CIRP, Volume 108, Pages 734-739, 2022.

[5] Maradia, U., Wegener, K. .EDM Modelling and Simulation. Electrical Discharge Machining (EDM): Types, Technologies and Applications. Chapter 3, pp.67-121, 2015.

[6] B. Izquierdo, J.A. Sánchez, S. Plaza, I. Pombo, N. Ortega, A numerical model of the EDM process considering the effect of multiple discharges, International Journal of Machine Tools and Manufacture, Volume 49, Issues 3–4, Pages 220-229, 2009.

[7] Feng, X., Wong, Y., Hong, G. (2016). Characterization and modeling of single and overlapping crater shapes in micro-EDM. Machining Science and Technology, Vol.20, pp 79-98 2016.

[8] Hinduja, S., Kunieda, M. Modelling of ECM and EDM processes. CIRP Annals - Manufacturing Technology 62 (2013) 775–797

[9] Kunieda M, Nakashima T. Factors Determining Discharge Location in EDM. IJEM No.3, pp. 53–58, 1998.

[10] Schumacher BM (1990) About the Role of Debris in the Gap During Electrical Discharge Machining. Annals of the CIRP 39(1):197–199.

[11] Kenji Morimoto, Masanori Kunieda, Sinking EDM simulation by determining discharge locations based on discharge delay time, CIRP Annals, Volume 58, Issue 1, Pages 221-224, 2009.

[12] Bai Shao, Kamlakar P. Rajurkar, Modelling of the Crater Formation in Micro-EDM, Procedia CIRP, Volume 33, Pages 376-381, 2015.

[13] Xiaodong Yang, Jianwen Guo, Xiaofei Chen, Masanori Kunieda, Molecular dynamics simulation of the material removal mechanism in micro-EDM, Precision Engineering, Volume 35, Issue 1, Pages 51-57, 2011.

[14] Borges Esteves, P., Wiessner, M., Costa, J., Sikora, M., Wegener, K. WEDM single crater asymmetry. The International Journal of Advanced Manufacturing Technology. Vol 117, pp 2421-2427. 2021.

[15] K. T. P. Tee, R. Hoseinnezhad, M. Brandt, J. Mo. Gap width control in electrical discharge machining, using type-2 fuzzy controllers. In 2013 International Conference on Control, Automation and Information Sciences (ICCAIS), pages 140–145. IEEE, 2013.

[16] S. T. Almeida, J. Mo, C. Bil, S. Ding, X.Wang. Servo control strategies for vibrationcontrol in robotic wire edm machining. Archives of Computational Methods in Engineering, 29(1):113–127, 2022.

[17] M. Yan, Y. Liao. Adaptive control of the wedm process using the fuzzy control strategy. Journal of Manufacturing Systems, 17(4):263–274, 1998.

[18] Y. Liao, J. Woo. Design of a fuzzy controller for the adaptive control of wedm process. International Journal of Machine Tools and Manufacture, 40(15):2293–2307, 2000.

[19] W. Lee, Y. Liao. Adaptive control of the wedm process using a self-tuning fuzzy logic algorithm with grey prediction. The International Journal of Advanced Manufacturing Technology, 34(5):527–537, 2007.

[20] G. Huang, W. Xia, L. Qin, W. Zhao. Online workpiece height estimation for reciprocated traveling wire edm based on support vector machine. Procedia CIRP, 68:126–131, 2018.